International Journal of Engineering Trends and Technology
ISSN: 2231–5381 / https://doi.org/10.14445/22315381/IJETT-V71I11P215

Volume 71 Issue 11, 136-147, November 2023

Original Article

Mechanical and Tribological Performance of Polyetheretherketone Composites using Tabletop 3D Printer

Taiwo Lolade Ladipo[1], Leonard Masu[2], Patrick Nziu[3]

[1,2,3]*Department of Industrial Engineering, Operation Management and Mechanical Engineering, Vaal University of Technology, South Africa.*

[1]*Corresponding Author: 220113106@edu.vut.ac.za*

Received: 12 July 2023 Revised: 07 September 2023 Accepted: 21 October 2023 Published: 04 November 2023

Abstract *- This article investigates the mechanical and tribological properties of 3D-printed Polyetheretherketone (PEEK) composites containing Molybdenum disulphide MoS2 and graphite fillers. 7 filament strands were created with varying weight percentages to print 35 dog bones and 7-disc samples for further analysis. The results showed a 61% increase in tensile strength of MoS2-filled PEEK (MoS2/PEEK) composite compared to plain PEEK. The filled PEEK had a reduced frictional response time and an average coefficient of friction of about 36% and 69 %, respectively. MoS2/PEEK showed superior wear resistance of about 50% compared to graphite-impregnated PEEK (Gr./PEEK).*

Keywords *- FFF printing, Graphite, MoS2, PEEK composites, Solid lubricants.*

1. Introduction

In the current time of Industry 4.0, there has been a lack of significant progress in innovative manufacturing techniques, thus paving the way for revolutionary opportunities in product design and the achievement of unparalleled efficiencies in the production process. Although traditional manufacturing methodologies have often been celebrated for their ability to achieve impressive production rates, meticulous control over material characteristics, and cost-effectiveness, there has been a simultaneous increase in the importance of Additive Manufacturing (AM), thus supplementing and enhancing the existing manufacturing landscape. [1-5] AM is a revolutionary technology transforming traditional product design and manufacturing methods. Through the progressive stacking of material, three-dimensional items are constructed from a computer-aided design model, giving professionals more geometrical freedom and design flexibility. This process provides greater design freedom and complexity, reduction of waste material, cost efficiency and faster production time compared to traditional manufacturing methods. [1, 2, 6–11] Major AM technology includes Material Extrusion (MEX.), Vat polymerisation, Laser Sinster (SLS or EBM), and Binder jetting. [5, 9, 10, 12-20]

The Stratasys corporation patented a MEX technique called Fused Deposition Modelling (FDM) or Fused filament fabrication (FFF), which creates 3D objects by depositing layers of melted thermoplastic material. The process's key parameters include layer height, nozzle diameter, printing speed, and extrusion temperature. [21–24] The MEX technique offers several advantages. It is a cost-effective 3D printing technique, making it accessible to many users. It supports various thermoplastic materials, allowing users to choose based on specific requirements. The process is user-friendly and does not require extensive training. Additionally, material extrusion enables the creation of support structures for printing complex geometries. [1, 12, 18, 25-27].

Visible layer lines called lamination may be present, requiring additional post-processing for smoother finishes. The layer-by-layer construction can result in lower strength compared to other methods. The MEX method is slower and has size restrictions, limiting large-scale production. Removing support structures can be challenging for intricate designs, potentially requiring manual effort and tools. [5, 28, 29] MEX. technique has gained popularity among various additive manufacturing techniques due to its cost-effectiveness and ease of use [30]. FFF, which uses a thermoplastic filament as a raw material, is one of the most appreciated additive manufacturing techniques. [26, 31, 32] The inherent advantages of the FFF process, including affordability, speed, and ease of use, make it an attractive method for manufacturing high-performance components using plastic composite. [15-17]

In the polymer domain in AM trends, producing functional components requires using a semi-crystalline polymer to modify material properties across a wide range, varying from the best mechanical and thermal to the lowest. This prerequisite renders commonly employed materials for AM, such as ABS and nylon, unsuitable due to their classification as lower-temperature plastics. PLA, another frequently employed material in AM, is a semi-crystalline polymer; however, its level of crystallinity and thermal resistivity is relatively low, and the range of temperature within which its crystalline characteristics can be altered is restricted, thereby rendering it unsuitable for the creation of a demonstrable AM functionally graded material (FGM). [1, 33–35]

Furthermore, studies have indicated that components manufactured through the FFF process using filled polymers exhibit enhanced mechanical performance and have the potential to acquire novel and improved attributes that are not observed in unfilled polymers or conventional production methods. [23, 36–39]. It is generally known that compositing polymers with fibre can affect properties like resistivity and other electrical properties; therefore, modification should be considered for a target set of material properties while sacrificing some.

PEEK composite is a favoured choice in contemporary MEX manufacturing assignments due to its exceptional mechanical and chemical attributes. The crystal arrangement of semi-crystalline polymers like PEEK is easily altered by the reheating that occurs during the MEX techniques, which makes the filling procedure involving the impregnation of the polymer easier than other plastics. [23, 40-42]

However, it is noted that MEX production in an open structure can be complex due to the high heat temperature requirement of PEEK composites, as most MEX printers' nozzles are made of low-temperature plastic like PLA. [1, 2, 43, 44] Incorporating a solid lubricant into PEEK, which possesses a high melt viscosity and is prone to extrusion and printing issues, can effectively mitigate the viscosity-related concerns at the nozzle. However, this addition also introduces alterations to the properties of the resulting printed parts. These incorporations will alter the tensile properties and tribological characteristics. [37, 45-48]

In some recent studies on MEX-PEEK, there has been a lack of investigations into the tribological characteristics of MEX's PEEK composites, with particular oversight of the influence of filler materials, such as solid lubricants, on the mechanical and tribological properties of these composites. Therefore, this research aims to examine and explain how different solid lubricants and their quantities affect the tribological behaviour of MEX-produced PEEK composites, as well as comprehensively analyse the impact of solid lubricants on the mechanical properties of these composites.

2. Materials and Methods

2.1. Sample Preparation

Inorganic graphite (Gr.), Molybdenum disulfide (MoS2), and PEEK 45) nanoparticles, with mean diameters of 45 µm, 100 µm, and 150 µm, respectively, were provided by Kayla Africa, a supplier and distributor at the Vaal University of Technology. The matrix (PEEK) 450, which was delivered by Kayla Africa, a supplier and distributor, comes with a data sheet that includes the following information: an average molecular weight (Mw) of 44,000 g⁄mol, a glass temperature (Tg) of 143 ºC, and a melting temperature (Tm) of 343 ºC. A particle size distribution analysis was conducted for each powder to confirm that the supplied powder was below 300 microns to avoid agglomeration.

Each of the solid lubricants, specifically Molybdenum disulphide (MoS2) and graphite (Gr), with varying volumes of 3 wt%, 5 wt%, and 10 wt%, were incorporated into the PEEK material in distinct manners utilising a mechanical mixer as illustrated in Figure 1. Figure 1 further shows the process chart used in filament production for this experiment. The initial step involved the mechanical mixing process, which facilitated the uniform dispersion of the lubricants throughout the PEEK matrix using the mechanical blender. Subsequently, this homogenised mixture was extruded into filaments, ensuring the consistent distribution of the lubricant. The powder created due to the mixing and blending process was further transformed into a filament through a Filastruder filament-making machine. Modifications were conducted on the Filastruder to enhance its performance by replacing the default PTFE-insulated Type K thermocouple with an E3D glass fibre-insulated Type K Cartridge Thermocouple, enabling the machine to operate at a temperature higher than its designated limit. The filament extrusion setup involving the Filastruder and Filawinder is shown in Figure 3(b).

Additionally, the power supply input was increased from 12 volts to 20 volts, thereby enhancing the heating capacity of the filament maker extruder. To minimise the impact of die swelling, the Filastruder underwent PID-tuning, which involved adjusting its parameters to effectively manage both the temperature and the torque, which refers to the speed at which the screw rotates during extrusion. A top table setup called Filawinder was employed to facilitate the filament reeling onto a spool. The Filawinder played a crucial role in mitigating die swelling by utilising an optical laser to monitor and rectify any variations in filament diameter. This was reached by modifying the stressing or compressing of the fibre in response to the speed of the engines. As for the Filastruder itself, it was configured to operate at the highest attainable temperature, reaching approximately 420^0C. This was executed using a single rotating screw and a nozzle diameter of 1.75 mm.

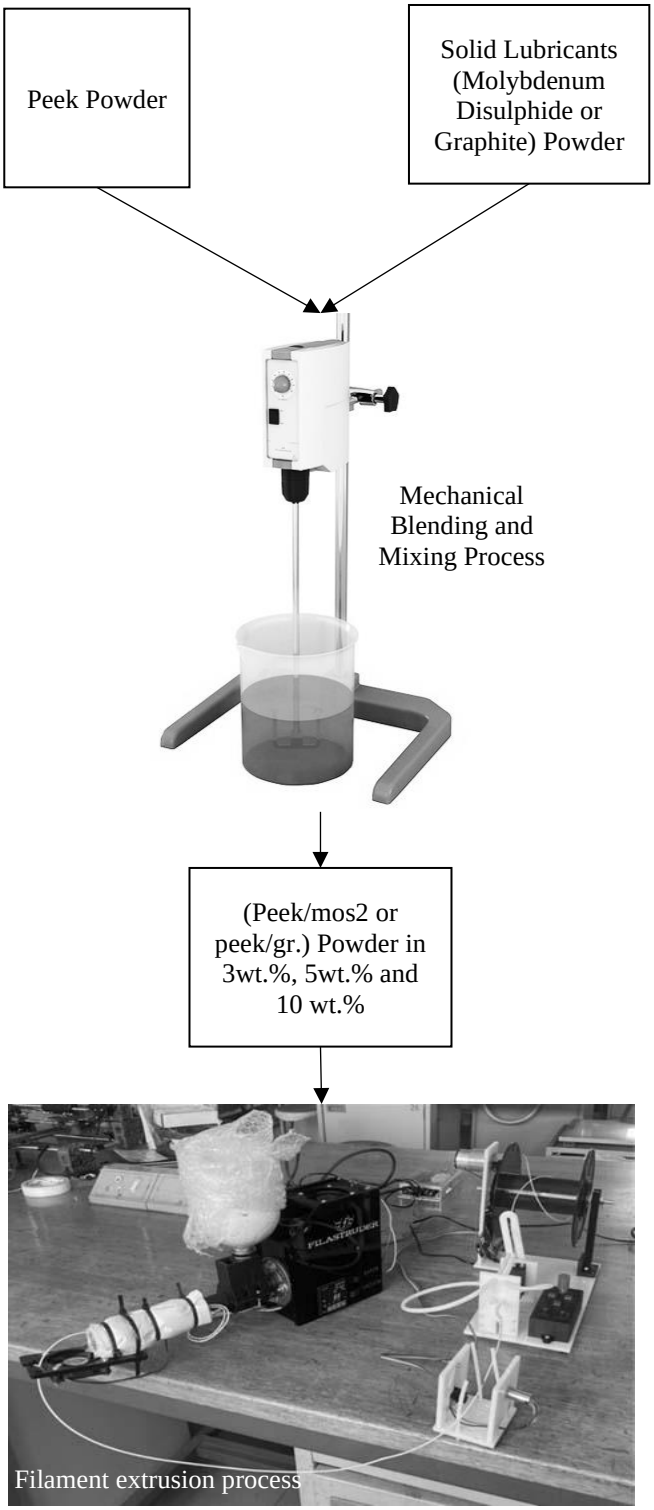

Fig. 1 Process chart for filament production

A control filament composed entirely of pure PEEK was also subjected to the extrusion process. Subsequently, seven groups of filament strands were meticulously printed using a retrofitted MEX technology printer known as the Fabbster. To establish the printing parameters, the open-sourced 3D Printer Slic3r software was employed, and these parameters are meticulously documented in Table 1. It is worth mentioning that during the printing process, the heated printing bed maintained a constant temperature of 120 ºC, while the ambient room temperature remained at a consistent 23 ºC. To acquire a substantial sample size, five tensile dog bones were printed from each of the seven groups of filaments, ultimately resulting in the production of 35 specimens per Type 1 of the ASTM D638 standard for plastic tensile testing.[49] It is essential to mention that the build orientation and printing direction were strictly adhered to during this process. The resulting tensile dog bones obtained from this carefully orchestrated procedure can be observed in Figure 2.

Table 1. presents the printing parameters

Printing parameters	Value
Layer thickness Extrusion	300 µm
Raster angle	0º
Extrusion temperature	345 ºC± 20 ºC
Printing Speed	20 mm/s
External Perimeter	3
Infill density	80%

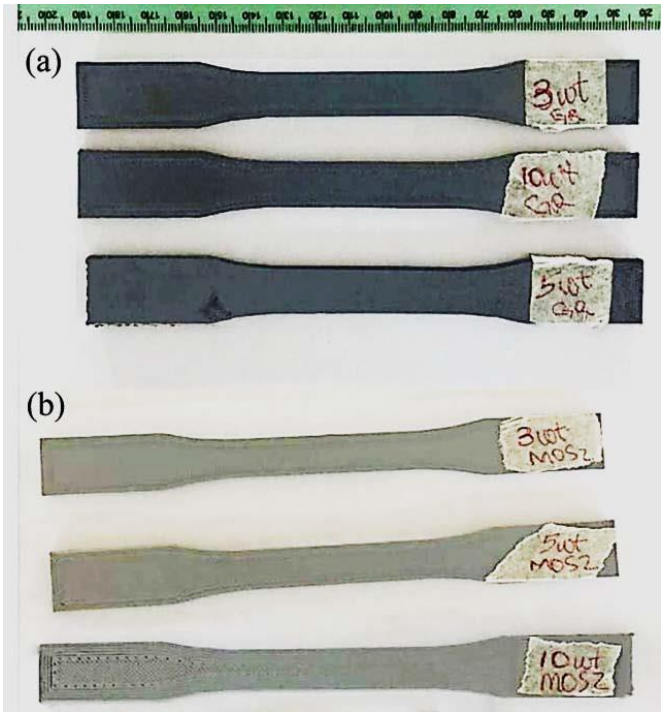

Fig. 2 Dog bone samples (a) graphite (b) MoS2

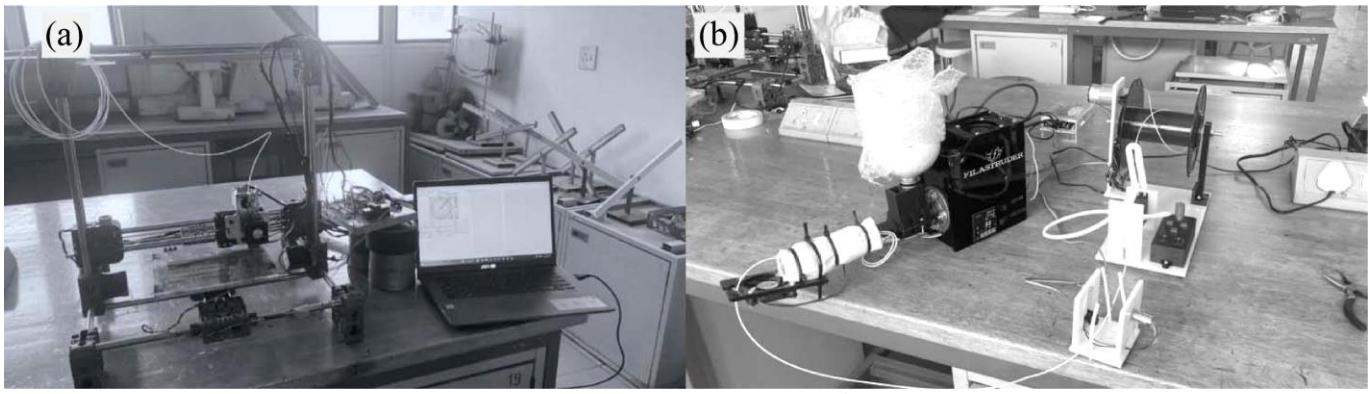

Fig. 3 (a) The altered Fabbster 3D printer during operation and (b) the filament extrusion and spooling setup

2.2. Printer Modification

The Fabbster 3D printer was modified to enable *pure and filled PEEK printing*. This was achieved by increasing the hot end temperature from 280°C to 470°C and setting the bed temperature to 150°C. The modifications included replacing the stock hot end with a micro-Swiss direct drive mounted on aluminium.

The printer's software was modified using VS-code with PlatformIO, and the firmware was edited from the Marlin 2 repository. *At the same time,* the control board was upgraded to the MKS Rumba 32-bit controller, allowing for heat bed configuration, high-temperature hot end, and sensor-less homing, eliminating the need for optical or mechanical end-stops, with the micro-stepping of the motors set to 1/32 for each axis, the motor current limited to 750 mA to prevent overheating of the stepper motors, and the *p*rinter's axes equipped with dual stepper motors, and sensorless homing activated using the TMC2226 driver.

The extrusion system of the printer was modified by replacing the Bowden tube style with a direct drive system using custom brackets, and a custom bracket was used to hang the micro-Swiss drive, resulting in a successful retrofitting of the printer for high-temperature PEEK printing with enhanced control and safety features.

Figure 3(a) depicts the altered Fabbster 3*D* printer while it is engaged in the intricate and complex process of printing, wherein layers upon layers of material are meticulously deposited to form the tensile dogbone.

2.3. Characterisation

The Mechanical tests were carried out using UTM by Inston 3369 with an extensometer, loaded with a cell of 30 kN as per ASTM D 638-14 test standards for plastics.[49] All the tensile properties were carried out at room temperature of 23 ^{o}C and 101.33 kPa and controlled displacement of a constant crosshead speed of 5 mm/min as per ASTM standard on plastics. The tensile strength, Elongation and young modulus were calculated using Instron software and exported as a CSV file.

Tribological properties were tested on the manufactured Samples per ASTM G99 in the Standard Test Method for Wear Testing with a Pin-on-Disk Apparatus.[50] The tribological test was carried out under a dry condition for an average of 1000 seconds at a speed of 3.5 ms^{-1} under a load of 10 N with a steel pin of diameter 6 mm as per ASTM G99 on the tribological test. The Coefficient of Friction was automatically plotted based on the friction response by the surface, and the wear rate was investigated using a mass scale and a tribometer per ASTM G99.

Table 2. Experimental average values of tensile strength, Elongation at break, and Young's modulus of the 3D printed plain PEEK and lubricant-filled PEEK composites

Composite	Averaged Tensile Strength (MPa)	Averaged Young's Modulus (GPa)	Averaged Elongation at Break (%)
Plain PEEK	96.9 ± 1.02	3.90 ± 0.217	26.59 ± 3.70
MoS2/PEEK 3wt.%	94.5 ± 0.90	3.95 ± 0.647	4.77 ± 0.45
MoS2/PEEK 5wt.%	98.6± 0.59	3.99 ± 0.527	4.80 ± 0.36
MoS2/PEEK 10wt.%	101.40 ± 1.64	4.48 ± 0.012	4.68 ± 1.32
Gr./PEEK 3wt.%	70.6 ± 0.47	3.99 ± 0.088	5.20 ± 0.31
Gr./PEEK 5wt.%	61.6 ± 4.53	4.16 ± 0.738	4.05 ± 0.20
Gr./PEEK 10wt.%	36.6 ± 0.65	4.49 ± 0.866	2.31 ± 0.9

3. Results and Discussion

3.1. Mechanical Properties

Table 1 presents the averaged values of Tensile properties of pure PEEK and loaded PEEK resulting from the experiment. The addition of Graphite to PEEK (Gr./PEEK) resulted in a non-linear decrease in tensile strength within the weight fraction range of 3% to 10%. Similarly, the Elongation at break exhibited a similar downward trend as the graphite fraction, depicted in Figure 4 and Figure 5.

In contrast, Young's modulus demonstrated a non-linear increase. The significant drop in Elongation at break can be attributed to the brittleness and agglomeration of graphite within the PEEK matrix, which is consistent with the finding of Chen et al. (2018). [51]

The declining tensile strength observed upon the addition of graphite can be attributed to the agglomeration of graphite particles within the PEEK matrix, possibly due to the substantial disparity in particle size and density between the two materials.

Moreover, the decrease in tensile strength may be influenced by the reduced adhesion forces between PEEK molecules and the further oxidation of graphite during filament production and printing. A sharp drop elongation was observed between 0 wt.% and 3 wt.% for both PEEK composites, followed by a gradual reduction.

The increasing presence of solid lubricants was associated with increased brittleness and weakened interfacial bonds within the PEEK matrix. Furthermore, the reinforcement of solids in PEEK may lead to reduced Elongation or crack initiation due to agglomeration.

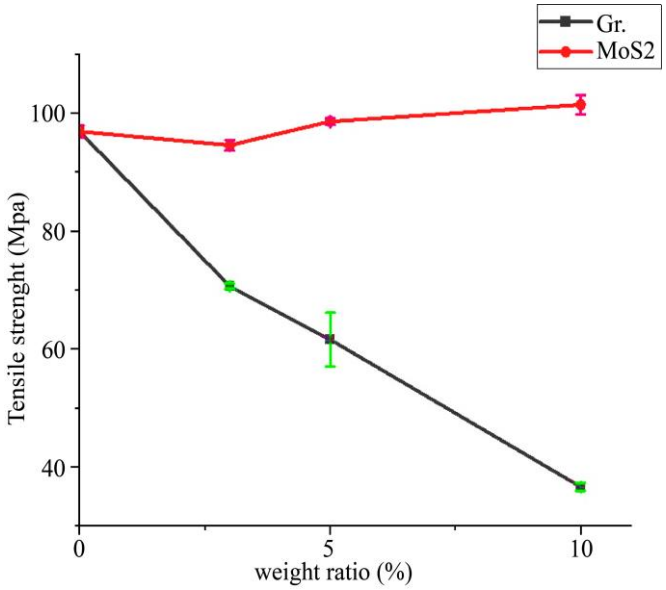

Fig. 4 Tensile Strength of PEEK, Gr/PEEK and MoS2/PEEK

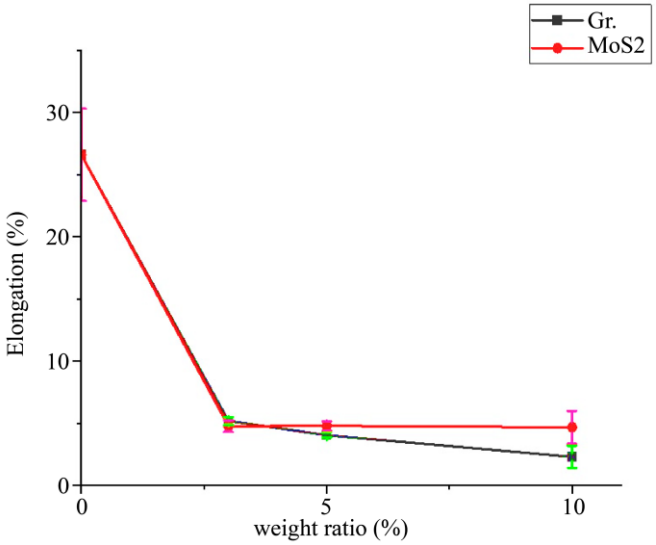

Fig 5 Elongation at break of PEEK, Gr/PEEK and MoS2/PEEK

On the other hand, the inclusion of MoS2 in PEEK (MoS2/PEEK) exhibited a non-linear increase in tensile strength and Young's modulus, reaching a maximum increase of 61%. This increase can be attributed to the uniform distribution of MoS2 within the PEEK matrix. Similar findings were reported in a study by Yan et al. on MoS2/PEEK. [52]

MoS2/PEEK demonstrated improved mechanical properties compared to PEEK/Gr. The highest recorded tensile strength was 101 MPa for a 10 wt.% MoS2 infill. Incorporating the two solid lubricants in 3D-printed PEEK has distinct effects on tensile strength. However, it should be noted that the experimental tensile strength exhibited a slight reduction compared to the known theoretical values, which is consistent with the trend observed in other studies on 3D-printed polymers. This reduction in tensile strength was attributed to the inherent characteristics of 3D-printed objects, which typically exhibit 70% to 80% of the tensile strength of traditionally fabricated counterparts. [53, 54]

Young's modulus, representing the ratio of stress to strain with an elastic limit, also exhibited distinct behaviour in response to the two solid lubricants. Figure 6 illustrates the reaction of PEEK to the two solids, with the control 3D-printed PEEK having a modulus of elasticity of 3.89 GPa. Gr/PEEK showed a nearly linear increase in Young's modulus as the additive fraction increased. In contrast, Young's modulus for MoS2/PEEK reached a plateau between 3 wt.% and 5 wt.%. The addition of solid lubricants increased the matrix of PEEK, resulting in a consistent increase in the elastic modulus of the printed PEEK composite. The highest recorded modulus values were 4.49 GPa for Gr./PEEK and 4.48 GPa for MoS2/PEEK at a 10 wt.% filler content, surpassing the control sample. This increase can be attributed to the stiffness of the solids, which enhances as solids increase.

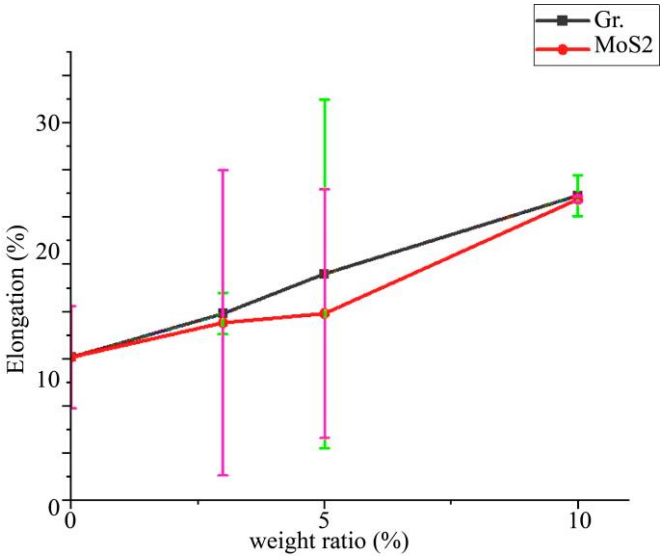

Fig. 6 Young's Modulus of PEEK, Gr/PEEK and MoS2/PEEK

Adding MoS2 to PEEK enhances stress strength when the loading surpasses 3 wt.%, likely because of MoS2's higher matrix density and better dispersion within PEEK. In contrast, graphite fillers show a consistent decline in strength, suggesting agglomeration within the PEEK matrix. Chen et al. (2018) and Fu et al. (2008) indicated that graphite addition exceeding 0.3 wt.% in PEEK leads to accumulation, resulting in weaker bonds and reduced fatigue resistance. [51, 55] Further research by Fu et al. (2008) highlighted the significance of matrix interfacial adhesion in determining the tensile strength of polymer composites, as it influences the effectiveness of stress transfer between fillers and the polymer. MoS2/PEEK exhibits improved stress strength, possibly due to its higher matrix density and dispersion, while graphite fillers tend to agglomerate, weakening the material.[56] The interfacial adhesion between the matrix and fillers plays a crucial role in the overall tensile strength of composite materials.

Albano et al. (2011) proposed various models to validate mechanical properties; one was Einstein's model from 1905 in Equation. 1 assumes that perfect adhesion and dispersion between fillers and polymer determines the effective shear viscosity.[55] The Einstein equation was simplified and modified into Guth and Smallwood's model in Equation 2. Guth's mathematical model suggests a linear relationship between the young modulus and viscosity for filler volume fractions less than 10%. Whilst a quadratic relationship is observed for higher loadings. The interaction and iteration of the models with experimental data of MoS2/PEEK and Gr./PEEK were graphically presented in Figure 7. Guth's work indicates that the tensile strength initially decreases at low filler fractions due to stress concentration. Equation 3 is the Boundary condition of modulus derived from the Voigt-Reuss model on a filled composite.

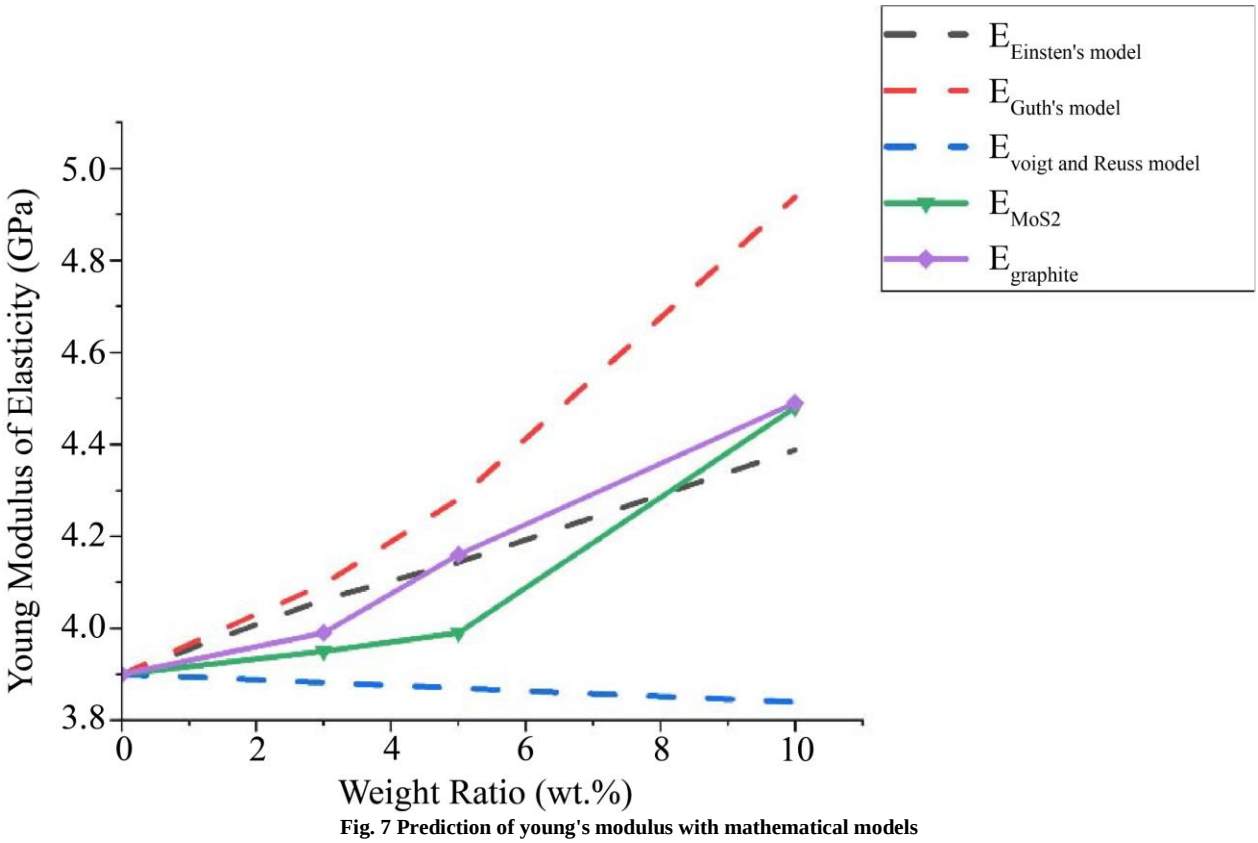

Fig. 7 Prediction of young's modulus with mathematical models

$$\frac{E_C}{E_m} = 1 + 1.25V_f \quad (1)$$

$$\frac{E_c}{E_m} = 1 + 2.5V_f + 14.1V_f^2 \quad (2)$$

$$E_c = E_m V_m + E_f V_f \quad (3)$$

Where E_m is the Modulus of unfilled Polymer, E_c is the Modulus of the filled Composite, and V_f is the Volume fraction of fillers.

Fu et al. (2008) found that the modulus of elasticity increases linearly with filler loading, regardless of interfacial adhesion. [56] The Nielsen model in Equation 4 explains the rapid decrease in Elongation at the break with increasing filler content and predicts enhanced tensile strength for perfect adhesion cases seen in Figures 4 and 5.

$$\varepsilon_c = \varepsilon_m(1 - V_f^{\frac{1}{3}}) \quad (4)$$

Where ε_c , ε_m and V_f are the Elongation at break for filled composite, Elongation at break for unfilled polymer, and volume fraction of fillers, respectively.

3.2. Tribology Properties

The average Coefficient of Friction (COF) of plain PEEK is around the nominal value of 0.25, indicating its weak capacity to minimise friction. This finding is consistent with previous research conducted by Zalaznik et al. (2016) and Yan et al. (2020). [52, 57]

The initial 300 seconds of testing were considered unreliable as the friction properties of impregnated PEEK stabilised after that.

Similarly, Yan et al. (2020) observed that the response time for PEEK implanted with MoS2 stabilises at approximately 350 seconds, while for PEEK alone takes about 950 seconds, as shown in Figures 8 and 9.

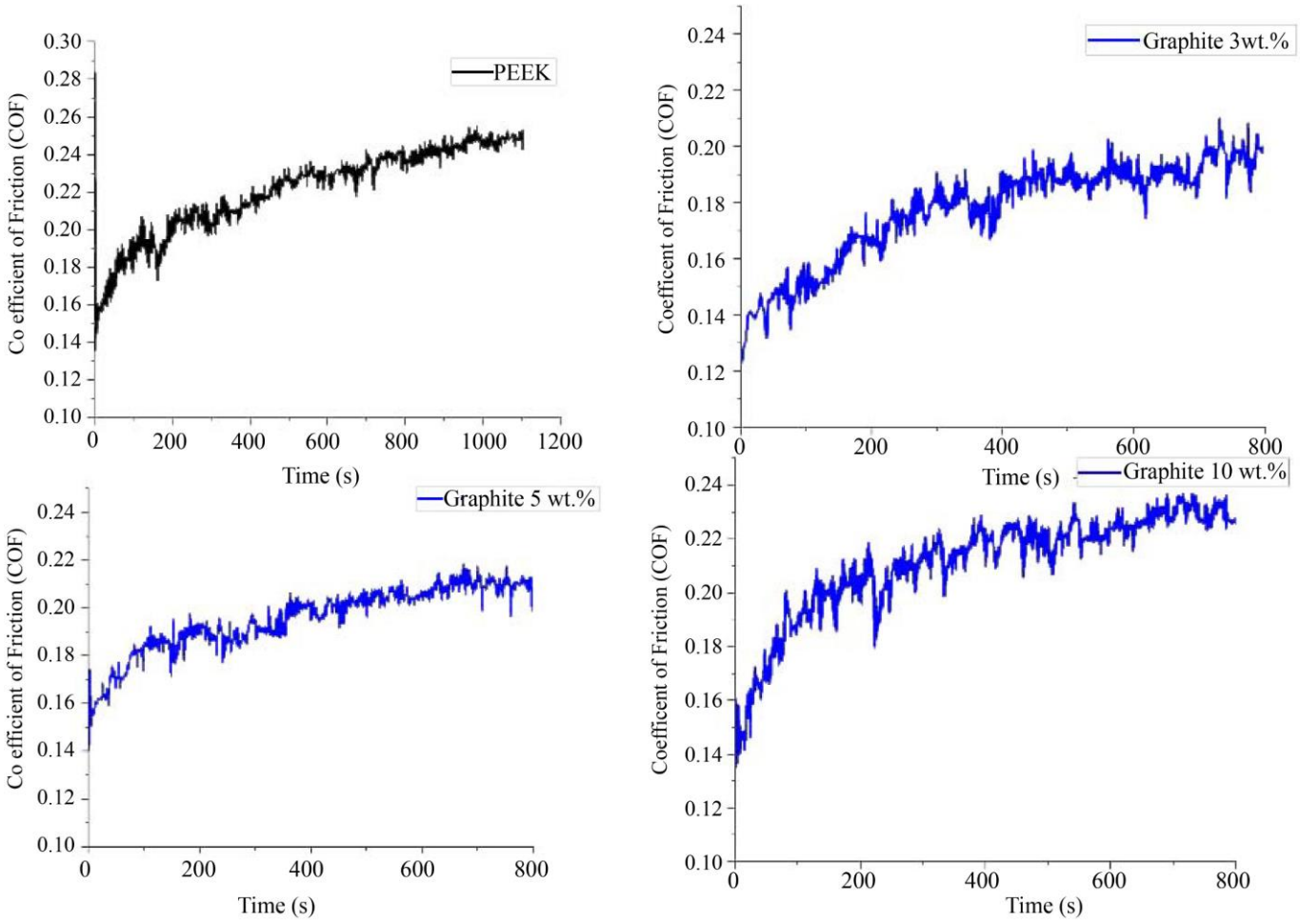

Fig. 8 The COF of Gr./PEEK in real-time response

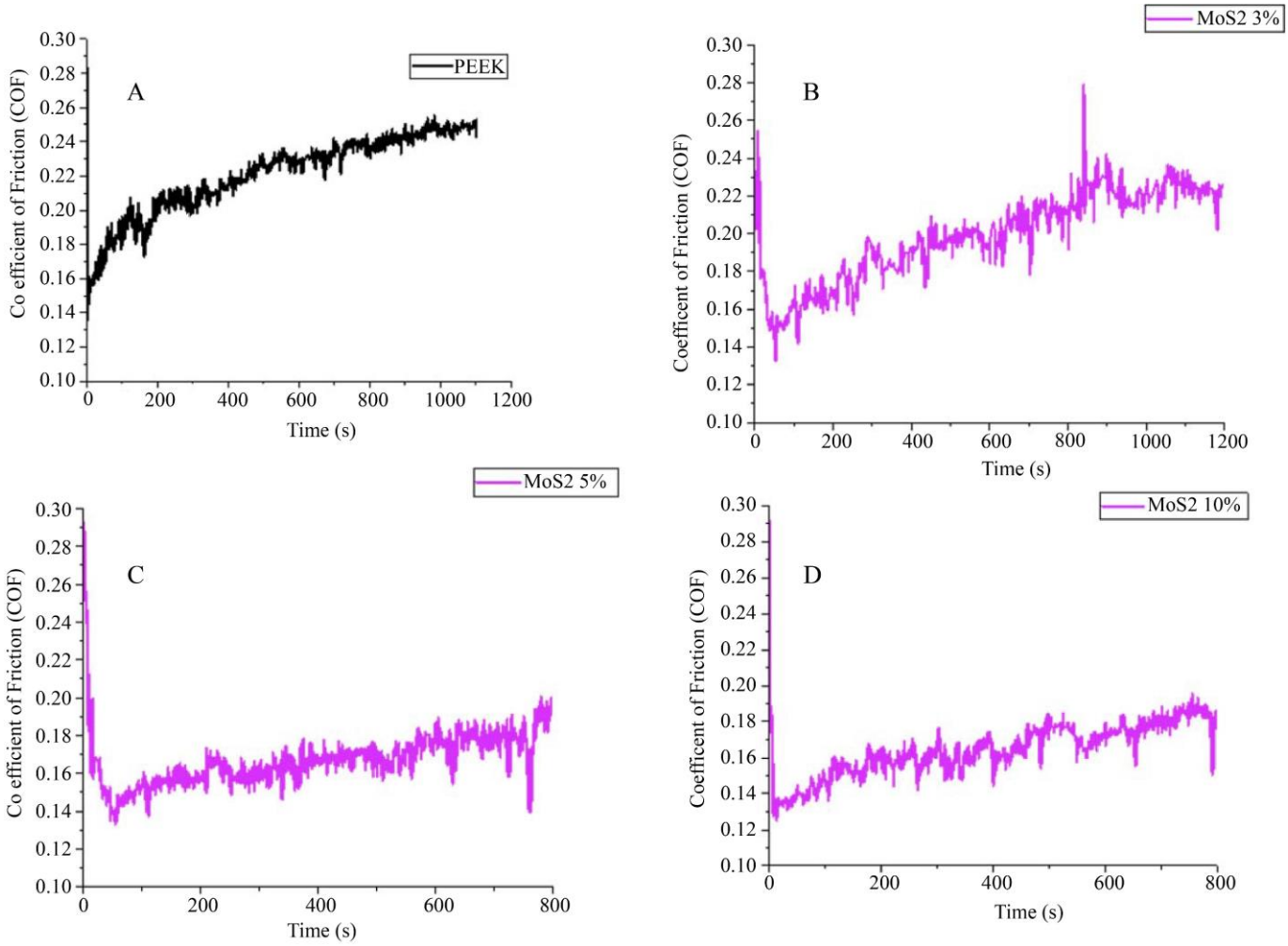

Fig. 9 The COF of MoS2. /PEEK in real-time response

Table 3. The average coefficient of friction and volume loss composite

Composite	Coefficient of Friction	Volume Loss (mm^3)
Plain PEEK	0.251	0.05362
MoS2/PEEK 3wt.%	0.213	0.02246
MoS2/PEEK 5wt.%	0.178	0.02934
MoS2/PEEK 10wt.%	0.171	0.03761
Gr./PEEK 3wt.%	0.217	0.03322
Gr./PEEK 5wt.%	0.219	0.04866
Gr./PEEK 10wt.%	0.223	0.09086

Adding MoS2 to the PEEK matrix gradually lowers the average COF, as seen in Figure 10 and Table 3, as confirmed by the trends discovered by Zalaznik et al. (2016). [57, 58] The self-lubrication properties of MoS2 contribute to the significant reduction in the average COF. Additionally, the low hardness, strong adhesion of particles, poor heat dissipating properties, and susceptibility to plastic deformation of unfilled PEEK contribute to its high COF. The wear volume of MoS2/PEEK is lower than that of Gr./PEEK, primarily due to the density of the crystal matrix. However, when graphite loading exceeds 5 wt.%, the volumetric Wear of PEEK increases due to the agglomeration of graphite particles within the matrix.

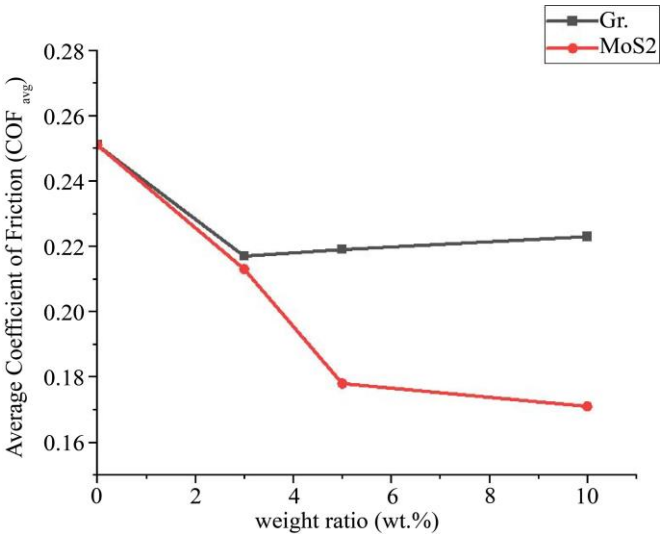

Fig. 10 The COF and weight ratio of solid lubricants

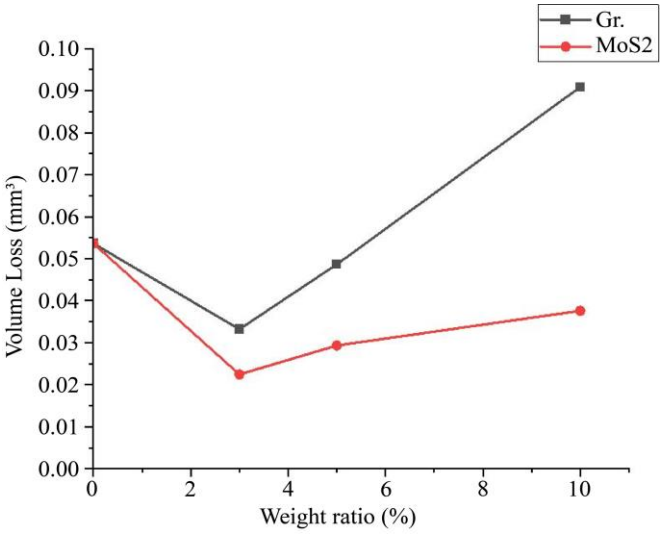

Fig. 11 The wear rate of Gr./PEEK and MoS2/PEEK

In contrast, adding MoS2 to PEEK reduces wear volume, especially at higher weight content, likely due to improved dispersion or thermal capacity. The trends of MoS2/PEEK and Gr./PEEK in terms of wear rate are depicted in Figure 11 and Table 3. The MoS2/PEEK composite shows a relative reduction in volumetric Wear at higher loading than the graphite-filled counterpart. The wear rate of 3D-processed PEEK initially decreases with the addition of both solid lubricant loadings, but it eventually stabilises after the further introduction of the fillers, following the trends of Elongation.

4. Conclusion

The following conclusions were drawn based on the findings of this study:

- In general, MoS2-filled PEEK showed the highest tensile strength, approximately 104 MPa at 10 wt.%. On the other hand, graphite-filled PEEK exhibited the lowest tensile strength, with a value of approximately 36 MPa at the same concentration. It is worth noting that these values represent the highest and lowest tensile strengths recorded in the experiment.
- The Elongation at failure dropped after adding both lubricants. The MoS2-lubricated PEEK showed an almost plateaued effect at about 4.7% elongation for 10 wt.%. In contrast, the graphite lubricated showed a further decline in Elongation to about 2.3% for 10 wt.%
- The modulus of elasticity result obtained from the experiment followed the linear upward trend as predicted by both Esitein and modified Guth models on the mechanical properties of the composite.
- Young's modulus of elasticity of MoS2-filled PEEK recorded the lowest value of 3.95 GPa at 3 wt.%, which is lower than the 3.99 GPa graphite-filled PEEK at 3 wt.%.
- The addition of graphite and MoS2 particles in PEEK polymer by up to 10% wt reduces the composite's frictional response time and coefficient of friction.
- The printed loaded composite has the lowest reduction in wear rate, averaging 58% and 38% for a volume fraction of 3 wt.% for both MoS2 and graphite, respectively.
- The MoS2-filled PEEK resists wearing better than the graphite-filled PEEKs in the lattice of the PEEK due to massive agglomeration and poor graphite dispersion in PEEK.

Overall, the study highlighted the significance of solid lubricant content and dispersion in influencing the mechanical and tribological properties of 3D-printed PEEK composites.

Funding Statement

The Vaal University of Technology funded this study.

Acknowledgements

The authors wish to acknowledge the Department of Industrial Engineering & Operations Management and Mechanical Engineering at Vaal University of Technology for enabling this research.

References

[1] Tobias Ritter et al., "Design and Modification of a Material Extrusion 3D Printer to Manufacture Functional Gradient Peek Components," *Polymers*, vol. 15, no. 18, pp. 1-19, 2023. [CrossRef] [Google Scholar] [Publisher Link]

[2] Marie Doumeng et al., "A Comparative Study of the Crystallinity of Polyetheretherketone by Using Density, DSC, XRD, and Raman Spectroscopy Techniques," *Polymer Testing*, vol. 93, 2021. [CrossRef] [Google Scholar] [Publisher Link]

[3] D.K.Y. Tam et al., "High-Performance Ballistic Protection Using Polymer Nanocomposites," *Advances in Military Textiles and Personal Equipment*, pp. 213-237, 2012. [CrossRef] [Google Scholar] [Publisher Link]
[4] Ali Bagheri, and Jianyong Jin, "Photopolymerization in 3D Printing," *ACS Applied Polymer Materials*, vol. 1, no. 4, pp. 593-611, 2019. [CrossRef] [Google Scholar] [Publisher Link]
[5] Mary Kathryn Thompson et al., "Design for Additive Manufacturing: Trends, Opportunities, Considerations, and Constraints," *CIRP Annals*, vol. 65, no. 2, pp. 737-760, 2016. [CrossRef] [Google Scholar] [Publisher Link]
[6] Nekoda van de Werken et al., "Additively Manufactured Carbon Fiber-Reinforced Composites: State of the Art and Perspective," *Additive Manufacturing*, vol. 31, 2020. [CrossRef] [Google Scholar] [Publisher Link]
[7] A.B. Baumgarten et al., "Investigation of Molybdenum Disulfide and Tungsten Disulfide as Additives to Coatings for Foul Release Systems," *Reclamation: Managing Water in the West*, pp. 1-14, 2011. [Google Scholar]
[8] Ian Gibson, David Rosen, and Brent Stucker, *Additive Manufacturing Technologies*: *3D Printing, Rapid Prototyping, and Direct Digital Manufacturing*, 2nd ed., New York: Springer, vol. 9, no. 5, pp. 1-509, 2015. [CrossRef] [Google Scholar] [Publisher Link]
[9] Dirk Herzog et al., "Additive Manufacturing of Metals," *Acta Materialia*, vol. 117, pp. 371-392, 2016. [CrossRef] [Google Scholar] [Publisher Link]
[10] Mahesh Mani, Kevin W. Lyons, and S.K. Gupta, "Sustainability Characterisation for Additive Manufacturing," *Journal of Research of the National Institute of Standards and Technology*, vol. 119, pp. 419-428, 2014. [CrossRef] [Google Scholar] [Publisher Link]
[11] Jared Allison, Conner Sharpe, and Carolyn Conner Seepersad, "Powder Bed Fusion Metrology for Additive Manufacturing Design Guidance," *Additive Manufacturing*, vol. 25, pp. 239-251, 2019. [CrossRef] [Google Scholar] [Publisher Link]
[12] About Additive Manufacturing: Material Extrusion, Additive Manufacturing Research Group, 2020. [Online]. Available: https://www.lboro.ac.uk/research/amrg/about/the7categoriesofadditivemanufacturing/materialextrusion/
[13] Deon de Beer et al., "A South African Additive Manufacturing Strategy," *Department of Science and Technology Republic of South Africa*, pp. 1-92, 2016. [Google Scholar] [Publisher Link]
[14] About Additive Manufacturing: VAT Photopolymerisation, Loughborough University Website, 2020. [Online]. Available: http://www.lboro.ac.uk/research/amrg/about/the7categoriesofadditivemanufacturing/vatphotopolymerisation/
[15] About Additive Manufacturing: Material Jetting, Loughborough University Website, 2020. [Online]. Available: http://www.lboro.ac.uk/research/amrg/about/the7categoriesofadditivemanufacturing/materialjetting/
[16] About Additive Manufacturing: Sheet Lamination, Loughborough University Website, 2020. [Online]. Available: http://www.lboro.ac.uk/research/amrg/about/the7categoriesofadditivemanufacturing/sheetlamination/
[17] About Additive Manufacturing: Binder Jetting, Loughborough University website, 2020. [Online]. Available: http://www.lboro.ac.uk/research/amrg/about/the7categoriesofadditivemanufacturing/binderjetting/
[18] ASTM WK62867, New Guide for Additive Manufacturing - General Principles - Guide for Design for Material Extrusion Processes, 2020. [Online]. Available: https://additive-manufacturing-report.com/technology/additive-manufacturing-standards/
[19] ASTM F2792-12a, Standard Terminology for Additive Manufacturing Technologies, American Society for Testing and Materials International, 2015. [Online]. Available: https://www.astm.org/f2792-12a.html
[20] ASTM ISO/ASTM 52910-18, "Additive Manufacturing-Design-Requirements, Guidelines and Recommendations, American *Society for Testing and Materials International*, 2018. [CrossRef] [Google Scholar] [Publisher Link]
[21] M. Somireddy, C.V. Singh, and A. Czekanski, "Analysis of the Material Behavior of 3D Printed Laminates via FFF," *Experimental Mechanics*, vol. 59, no. 6, pp. 871-881, 2019. [CrossRef] [Google Scholar] [Publisher Link]
[22] Miguel Fernandez-Vicente, Miquel Canyada, and Andres Conejero, "Identifying Limitations for Design for Manufacturing with Desktop FFF 3D Printers," *International Journal of Rapid Manufacturing*, vol. 5, no. 1, pp. 116-128, 2015. [CrossRef] [Google Scholar] [Publisher Link]
[23] Muhamad F. Arif et al., "Multifunctional Performance of Carbon Nanotubes and Graphene Nanoplatelets Reinforced PEEK Composites Enabled via FFF Additive Manufacturing," *Composites Part B: Engineering*, vol. 184, 2020. [CrossRef] [Google Scholar] [Publisher Link]
[24] Vicente M. Rivas Santos et al., "Design and Characterisation of an Additive Manufacturing Benchmarking Artefact Following a Design-For-Metrology Approach," *Additive Manufacturing*, vol. 32, 2020. [CrossRef] [Google Scholar] [Publisher Link]
[25] S. Drücker et al., "Solid Epoxy for Functional 3D Printing with Isotropic Mechanical Properties by Material Extrusion," *Additive Manufacturing*, vol. 55, 2022. [CrossRef] [Google Scholar] [Publisher Link]
[26] Cleiton André Comelli et al., "PEEK Filament Characteristics Before and After Extrusion within Fused Filament Fabrication Process," *Journal of Materials Science*, vol. 57, no. 1, pp. 766-788, 2022. [CrossRef] [Google Scholar] [Publisher Link]
[27] K. Wilczyński, A. Tyszkiewicz, and Z. Szymaniak, "Modeling for Morphology Development During Single-Screw Extrusion of LDPE/PS Blend," *Journal of Materials Processing Technology*, vol. 109, no. 3, pp. 320-323, 2001. [CrossRef] [Google Scholar] [Publisher Link]
[28] Julien Gardan, "Additive Manufacturing Technologies for Polymer Composites: State-of-the-Art and Future Trends," *Structure and Properties of Additive Manufactured Polymer Components*, pp. 3-15, 2020. [CrossRef] [Google Scholar] [Publisher Link]

[29] S. Nithya Priya et al., "Design and Fabrication of Filament Extruder with Spooler," *Materials Today: Proceedings*, vol. 81, no. 2, pp. 221-223, 2023. [CrossRef] [Google Scholar] [Publisher Link]

[30] Sunil Khabia, and Kamlesh K. Jain, "Influence of Change in Layer Thickness on Mechanical Properties of Components 3D Printed on Zortrax M 200 FDM Printer with Z-ABS Filament Material and Accucraft i250+ FDM Printer with Low Cost ABS Filament Material," *Materials Today: Proceedings*, vol. 26, no.2, pp. 1315-1322, 2020. [CrossRef] [Google Scholar] [Publisher Link]

[31] Panagiotis M. Angelopoulos, Michail Samouhos, and Maria Taxiarchou, "Functional Fillers in Composite Filaments for Fused Filament Fabrication: A Review," *Materials Today: Proceedings*, vol. 37, pp. 4031-4043, 2019. [CrossRef] [Google Scholar] [Publisher Link]

[32] Disha Deb, J.M. Jafferson, "Natural Fibers Reinforced FDM 3D Printing Filaments," *Materials Today: Proceedings*, vol. 46, no. 2 pp. 1308-1318, 2021. [CrossRef] [Google Scholar] [Publisher Link]

[33] Seong Je Park, "3D Printing of Bio-Based Polycarbonate and its Potential Applications in Ecofriendly Indoor Manufacturing," *Additive Manufacturing*, vol. 31, 2020. [CrossRef] [Google Scholar] [Publisher Link]

[34] Hao Wu et al., "Recent Developments in Polymers/Polymer Nanocomposites for Additive Manufacturing," *Progress in Materials Science*, vol. 111, 2020. [CrossRef] [Google Scholar] [Publisher Link]

[35] Gayan Adikari Appuhamillage, "*New 3D Printable Polymeric Materials for Fused Filament Fabrication (FFF),*" Dissertation, The University of Texas at Dallas, pp. 1-112, 2018. [CrossRef] [Google Scholar] [Publisher Link]

[36] Leyu Lin et al., "Impact of Nanosilica on the Friction and Wear of a PEEK/CF Composite Coating Manufactured by Fused Deposition Modeling (FDM)," *Composites Part B: Engineering*, vol. 177, 2019. [CrossRef] [Google Scholar] [Publisher Link]

[37] P. Firoozian et al., "Prediction of Mechanical Properties of Mica-Filled Epoxy Composite Using Various Mechanical Models," *Journal of Reinforced Plastics and Composites*, vol. 29, no. 15, pp. 2368-2378, 2010. [CrossRef] [Google Scholar] [Publisher Link]

[38] Fang-long Yin, Hui Ji, and Song-lin Nie, "Tribological Behavior of Various Ceramic Materials Sliding Against CF/PTFE/Graphite-Filled PEEK under Seawater Lubrication," *Proceedings of the Institution of Mechanical Engineers, Part J: Journal of Engineering Tribology*, vol. 233, no. 11, pp. 1729-1742, 2019. [CrossRef] [Google Scholar] [Publisher Link]

[39] Vijay Tambrallimath et al., "Thermal Behavior of PC-ABS based Graphene Filled Polymer Nanocomposite Synthesised by FDM Process," *Composites Communications*, vol. 15, pp. 129-134, 2019. [CrossRef] [Google Scholar] [Publisher Link]

[40] Debashis Puhan, and Janet S.S. Wong, "Properties of Polyetheretherketone (PEEK) Transferred Materials in a PEEK-Steel Contact," *Tribology International*, vol. 135, pp. 189-199, 2019. [CrossRef] [Google Scholar] [Publisher Link]

[41] Sangram A. Sathe et al., "A Modified Cage Insertion Device For Transforaminal Lumbar Interbody Fusion Surgery," *SSRG International Journal of Pharmacy and Biomedical Engineering*, vol. 8, no. 2, pp. 6-10, 2021. [CrossRef] [Publisher Link]

[42] Pham Son Minh, and Tu Thi Tuyet, "Influence of 3D-Printing Parameters on Flexural Strength of PLA Plastic Products," *SSRG International Journal of Mechanical Engineering*, vol. 7, no. 3, pp. 1-4, 2020. [CrossRef] [Google Scholar] [Publisher Link]

[43] Eric McNiffe et al., "Advancements in Functionally Graded Polyether Ether Ketone Components: Design, Manufacturing, and Characterisation Using a Modified 3D Printer," *Polymers*, vol. 15, no. 14, pp. 1-15, 2023. [CrossRef] [Google Scholar] [Publisher Link]

[44] Atefeh Golbang et al., "Production and Characterisation of PEEK/IF-WS_2 Nanocomposites for Additive Manufacturing: Simultaneous Improvement in Processing Characteristics and Material Properties," *Additive Manufacturing*, vol. 31, 2020. [CrossRef] [Google Scholar] [Publisher Link]

[45] Maria Rosaria Caputo et al., "Influence of FFF Process Conditions on the Thermal, Mechanical, and Rheological Properties of Poly(Hydroxybutyrate-co-Hydroxy Hexanoate)," *Polymers*, vol. 15, no. 8, pp. 1-25, 2023. [CrossRef] [Google Scholar] [Publisher Link]

[46] Maciej Mrówka et al., "Mechanical, Chemical, and Processing Properties of Specimens Manufactured from Poly-Ether-Ether-Ketone (Peek) Using 3D Printing," *Materials*, vol. 14, no. 11, pp. 1-13, 2021. [CrossRef] [Google Scholar] [Publisher Link]

[47] Vishal Francis, and Prashant K. Jain, "Achieving Improved Dielectric, Mechanical, and Thermal Properties of Additive Manufactured Parts via Filament Modification Using OMMT-Based Nanocomposite," *Progress in Additive Manufacturing*, vol. 2, no. 3, pp. 109-115, 2017. [CrossRef] [Google Scholar] [Publisher Link]

[48] Leipeng Yang et al., "Effects of Carbon Nanotube on the Thermal, Mechanical, and Electrical Properties of PLA/CNT Printed Parts in the FDM Process," *Synthetic Metals*, vol. 253, pp. 122-130, 2019. [CrossRef] [Google Scholar] [Publisher Link]

[49] ASTM D638-14, "Standard Test Method for Tensile Properties of Plastics," *American Society for Testing and Materials International*, vol. 82, pp. 1-15, 2014. [CrossRef] [Google Scholar] [Publisher Link]

[50] ASTM G99-95a, "Standard Test Method for Wear Testing with a Pin-on-Disk Apparatus," *American Society for Testing and Materials International*, pp. 1-5, 2014. [CrossRef] [Google Scholar] [Publisher Link]

[51] Binling Chen et al., "A Primary Study into Graphene/Polyether Ether Ketone (PEEK) Nanocomposite for Laser Sintering," *Applied Surface Science*, vol. 428, pp. 1018-1028, 2018. [CrossRef] [Google Scholar] [Publisher Link]

[52] Yutao Yan et al., "Preparation and Tribological Behaviors of Lubrication-Enhanced Peek Composites," *Applied Sciences*, vol. 10, no. 21, pp. 1-15, 2020. [CrossRef] [Google Scholar] [Publisher Link]

[53] Aboma Wagari Gebisa, and Hirpa G. Lemu, "Influence of 3D printing FDM Process Parameters on Tensile Property of ULTEM 9085," *Procedia Manufacturing*, vol. 30, pp. 331-338, 2019. [CrossRef] [Google Scholar] [Publisher Link]

[54] Shilpesh R. Rajpurohit, and Harshit K. Dave, "Impact of Process Parameters on Tensile Strength of Fused Deposition Modeling Printed Crisscross Poylactic Acid," *World Academy of Science Engineering and Technology*, vol. 12, no. 2, pp. 1- 6, 2018. [CrossRef] [Google Scholar] [Publisher Link]

[55] C. Albano et al., "Prediction of Mechanical Properties of Composites of HDPE/HA/EAA," *Journal of the Mechanical Behavior of Biomedical Materials*, vol. 4, no. 3, pp. 467-475, 2011. [CrossRef] [Google Scholar] [Publisher Link]

[56] Shao-Yun Fu et al., "Effects of Particle Size, Particle/Matrix Interface Adhesion and Particle Loading on Mechanical Properties of Particulate-Polymer Composites," *Composites Part B: Engineering*, vol. 39, no. 6, pp. 933-961, 2008. [CrossRef] [Google Scholar] [Publisher Link]

[57] M. Zalaznik et al., "Tribological Behaviour of a PEEK Polymer Containing Solid MoS_2 Lubricants," *Lubrication Science*, vol. 28, no. 1, pp. 27-42, 2016. [CrossRef] [Google Scholar] [Publisher Link]

[58] M. Zalaznik et al., "Effect of the Type, Size and Concentration of Solid Lubricants on the Tribological Properties of the Polymer PEEK," *Wear*, vol. 364, pp. 31-39, 2016. [CrossRef] [Google Scholar] [Publisher Link]